



www.asianpubs.org

ARTICLE

PM3 Method based QSAR Study of the Derivatives of Thiadiazole and Quinoxaline for Antiepileptic Activity using Topological Descriptors

Durgesh Kumar Mishra¹, Ashutosh Singh²✉, Sunil Mishra¹, Priti Singh² and Abhishek Singh³

ABSTRACT

QSAR study of the derivatives of thiadiazole and quinoxaline has been performed for the antiepileptic activity using the topological descriptors viz., molar refractivity, shape index (basic kappa, order 1), shape index (basic kappa, order 2), shape index (basic kappa, order 3), valence connectivity index (order 0, standard), valence connectivity index (order 1, standard) and valence connectivity index (order 2, standard). In the best QSAR model, the descriptors are molar refractivity, shape index (basic kappa, order 1), shape index (basic kappa, order 3) and valence connectivity index (order 0, standard). In this QSAR model, the regression coefficient is 0.872435 and cross-validation coefficient is 0.832189, which indicate that this QSAR model can be used to predict the antiepileptic activity of any compound belonging to this series. QSAR model developed using single descriptor shape index (basic kappa, order 1) or shape index (basic kappa, order 3) or valence connectivity index (order 2, standard) also has good predictive power.

KEYWORDS

QSAR models, Thiadiazole, Quinoxaline, Descriptors, Antiepileptic activity, Computational chemistry.

INTRODUCTION

QSAR is a process in which the structures of a set of compounds are quantified and then compared to the numerical values of a biological activity or a physical property [1-5]. The challenge here has been to find some numerical code for a molecule or a fragment that is information-rich. This structure information and the measured property or activity is then processed into a mathematical model of relationship. From a good QSAR model, it is possible to predict and design the compounds for synthesis and testing that have a good possibility for activity [4-9].

Computational chemistry [10-16] represents molecular structures as a numerical model and simulates their behaviour with the equations of quantum and classical physics. Available programs enable scientists to easily generate and present molecular data including geometries, energies and associated properties. A QSAR attempts to find consistent relationships between the variations in the values of molecular properties

Asian Journal of Organic & Medicinal Chemistry

Volume: 7 Year: 2022
Issue: 1 Month: January–March
pp: 99–110
DOI: <https://doi.org/10.14233/ajomc.2022.AJOMC-P370>

Received: 10 February 2022

Accepted: 19 March 2022

Published: 5 April 2022

Author affiliations:

¹Department of Chemistry, M.L.K. Post Graduate College, Balrampur-271201, India

²Department of Chemistry, K.S. Saket Post Graduate College, Ayodhya-224123, India

³Department of Chemistry, Udai Pratap Autonomous College, Varanasi-221003, India

✉To whom correspondence to be addressed:

E-mail: asinghkssaket@gmail.com; dmchemistrydada@gmail.com

Available online at: <http://ajomc.asianpubs.org>

and the biological activity for a series of compounds.

A QSAR generally takes the form of a linear equation:

$$\text{Biological activity} = \text{Const} + (C_1 P_1) + (C_2 P_2) + (C_3 P_3) + \dots + (C_n P_n)$$

where the parameters P_1 through P_n are computed for each molecule in the series and the coefficients C_1 through C_n are calculated by fitting variations in the parameters and the biological activity [17-25].

EXPERIMENTAL

Molar refractivity [26]: Molar refractivity was calculated by the Lorenz-Lorentz formula:

$$\text{MR} = \frac{n^2 - 1}{n^2 + 1} \times \frac{M}{\rho}$$

where M is the molecular weight, n is the refraction index and ρ is the density. For a radiation of infinite wavelength, molar refractivity represents the real volume of the molecules.

Kier's shape indices $\{k_n (n = 1, 2, 3)\}$ [27-30,35]: These indices compare the molecule graph with "minimal" and "maximal" graphs, where the meaning of "minimal" and "maximal" depends on the order n . This is intended to capture different aspects of the molecular shape.

Order 1: The shape index of order 1 is then defined as:

$$\kappa_1 = 2P_{\min} \frac{P_{\max}}{P^2}$$

where P is the number of edges in the graph (edges are paths of length 1, hence the subscript on the κ_1), P_{\max} is the number of edges in the maximal graph namely $N(N-1)/2$ and P_{\min} is the number of edges in the minimal graph namely $(N-1)$.

By inserting the formulas for P_{\max} and P_{\min} , one obtains the implemented formula:

$$\kappa_1 = \frac{N(N-1)^2}{P^2} \quad (1)$$

Order 2: The descriptor k_2 encodes the branching. P , P_{\min} and P_{\max} now denote the number of paths of length 2 in the corresponding graphs. The maximal graph is taken to be the star graph in which all atoms are adjacent to a common atom. Thus, $P_{\max} = (N-1)(N-2)/2$. The linear graph is again taken as the minimal graph, so $P_{\min} = N-2$. eqn. 1 thus yields:

$$\kappa_2 = \frac{(N-1)(N-2)^2}{P^2} \quad (2)$$

Order 3: For order 3, the counts of paths of length 3 are considered and the maximal graph chosen is a twin-star with $P_{\max} = (N-1)(N-3)/4$ for N odd and $P_{\max} = (N-2)^2/4$ for N even. The minimal graph is again the linear one with $P_{\min} = N-3$.

The equation is adjusted by another factor of 2 in the words of the index design "to bring the values into rough equivalence with the other kappa values".

$$\kappa_3 = \frac{(N-1)(N-3)^2}{P^2} \text{ for } N \text{ odd}$$

$$\text{and } \kappa_3 = \frac{(N-2)(N-3)^2}{P^2} \text{ for } N \text{ even} \quad (3)$$

Valence connectivity indices: Valence connectivity indices are originally defined by Randić [34] and subsequently refined by Kier & Hall [35], is a series of numbers designated by "order" and "sub-graph type". There are four sub-graph types; path, cluster, path/cluster and chain. These types emphasize different aspects of atom connectivity within a molecule, the amount of branching, ring structures present and flexibility. It is calculated from the hydrogen suppressed molecular graph and defined as follows:

$${}^m\chi^v = \sum_{i=1}^{NS} \prod_{k=1}^{m+1} \left(\frac{1}{\delta_k^v} \right)^{1/2}$$

where, $\delta_k^v = \frac{(Z_k^v - H_k)}{(Z_k - Z_k^v - 1)}$ - valence connectivity for the k th

atom in the molecular graph, Z_k = the total number of electrons in the k th atom, Z_k^v = the number of valence electrons in the k th atom, H_k = the number of hydrogen atoms directly attached to the k th non-hydrogen atom, $m = 0$ - atomic valence connectivity indices (called order-0), $m = 1$ - one bond path valence connectivity indices (called order-1), $m = 2$ - two bond fragment valence connectivity indices (called order-2).

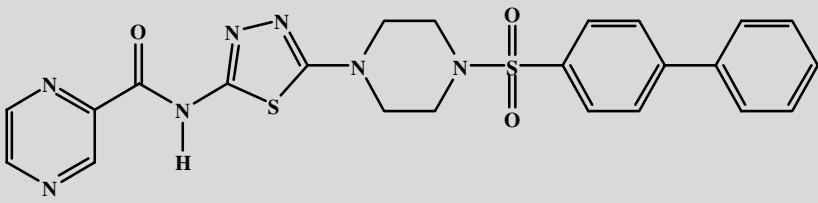
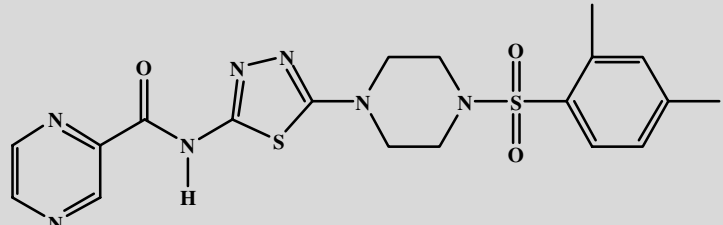
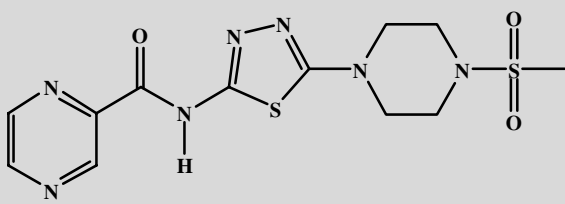
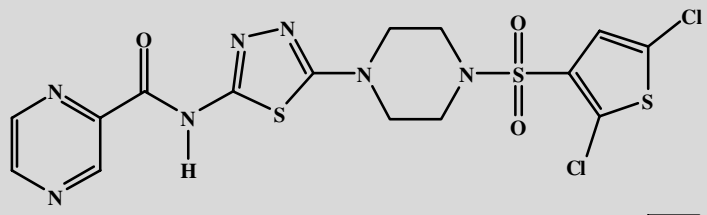
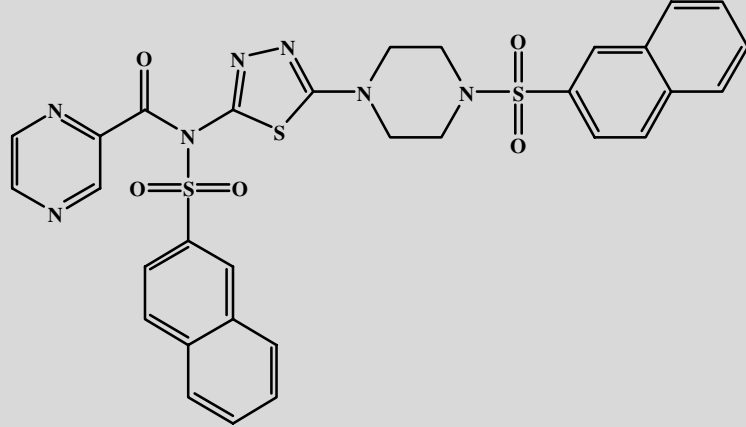
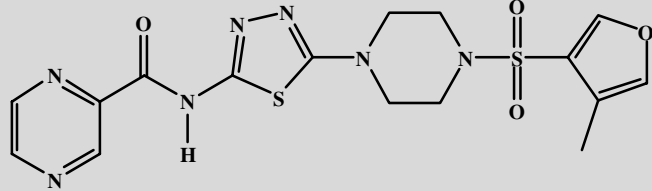
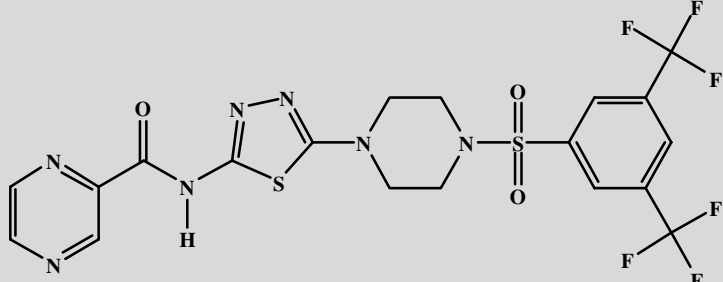
Study material: Derivatives of thiaziazole and quinoxaline have been used as the study material. These derivatives are presented in Table-1 along with their antiepileptic activities (pED_{50}). For QSAR analysis, the 3D modeling and geometry optimization [22,23] of all the compounds have been done with the help of CAChe software. The values of descriptors used for QSAR models have been evaluated using the CAChe software by PM3 [24,25] methods. The descriptors that have been used for the development of QSAR models are given below:

1. Molar refractivity
2. Shape index (basic kappa, order 1)
3. Shape index (basic kappa, order 2)
4. Shape index (basic kappa, order 3)
5. Valence Connectivity Index (order 0, standard)
6. Valence connectivity index (order 1, standard)
7. Valence connectivity index (order 2, standard)

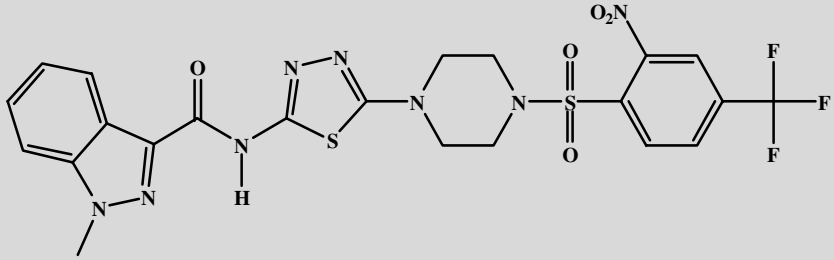
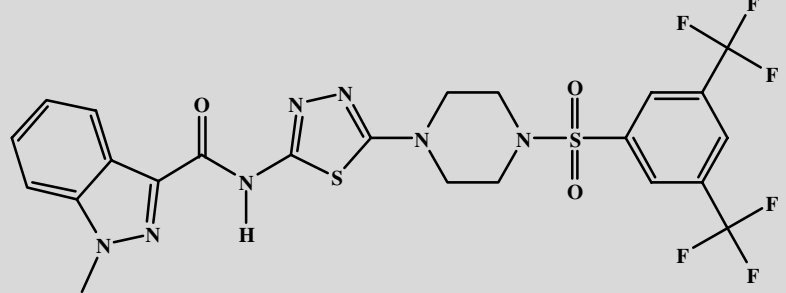
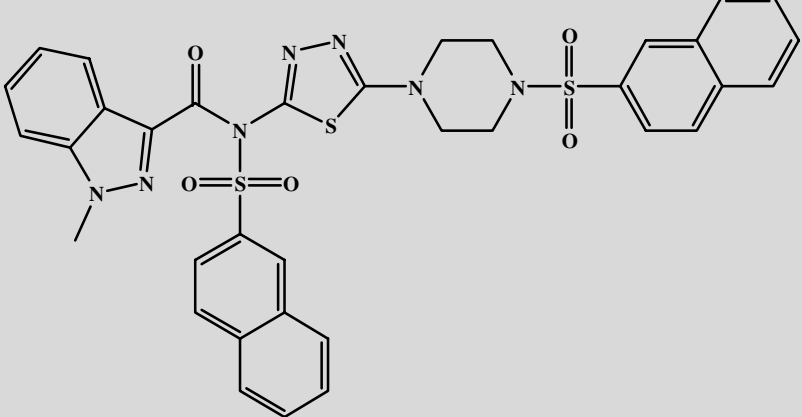
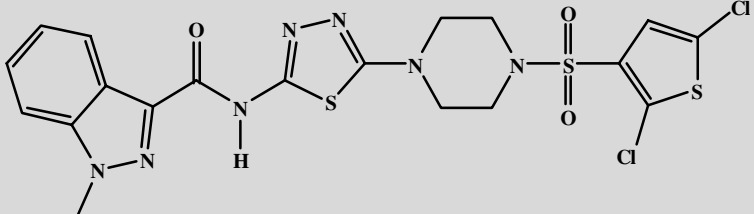
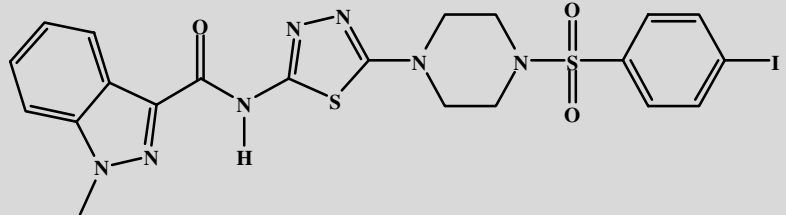
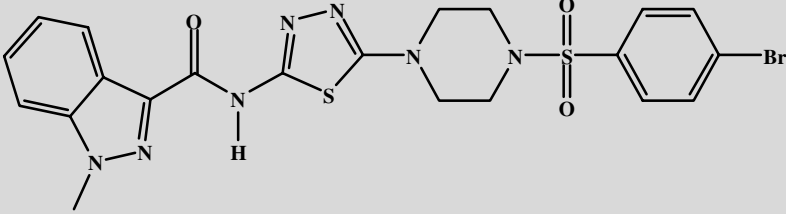
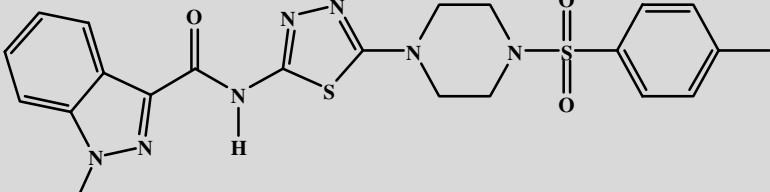
RESULTS AND DISCUSSION

QSAR studies of the compounds listed in Table-1 were made with the help of topological descriptors in the different combinations. The outlier compounds were TD14, TD23 and TD37. The values of the descriptors have been calculated using PM3 method with the help of CAChe software and are given in Table-2. The values of the descriptors have been used to develop ninety QSAR models using different combinations of descriptors. With the help of good QSAR models, the activity of any unknown compound of the series can be calculated and the then synthesis may be done if the activity is found good. A QSAR model is said to have good predictive power if the regression coefficient (r^2) is greater than 0.5 and the value of cross-validation coefficient (rCV^2) is greater than or equal to 0.2. As the value of regression coefficient increases, the predictive power of the QSAR model increases. A QSAR model is said to have 100% predictive power if the value of

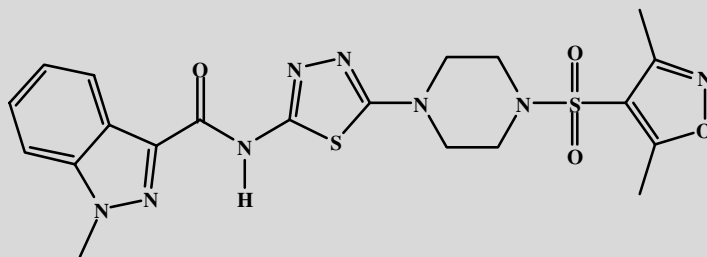
TABLE-1
 ANTIEPILEPTIC ACTIVITIES (pED₅₀) OF THIADIAZOLES AND QUINOXALINE DERIVATIVES

Compound	Compound structure	Antiepileptic activity (pED ₅₀)
TD 1		0.81
TD 2		0.87
TD 3		0.91
TD 4		0.30
TD 5		0.83
TD 6		0.54
TD 7		0.24

TD 8		0.90
TD 9		0.90
TD 10		0.40
TD 11		0.67
TD 12		0.91
TD 13		0.32
TD 14		0.65
TD 15		0.47

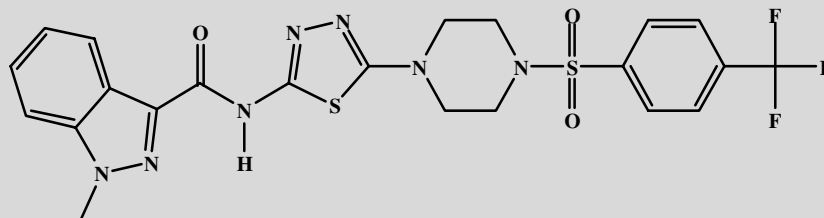
TD 16		0.33
TD 17		0.25
TD 18		0.81
TD 19		0.32
TD 20		0.80
TD 21		0.79
TD 22		0.84

TD 23



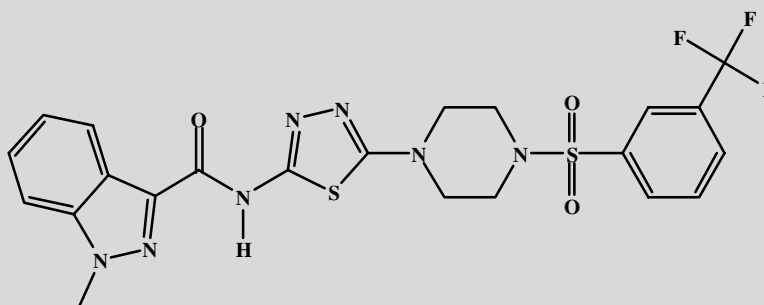
0.34

TD 24



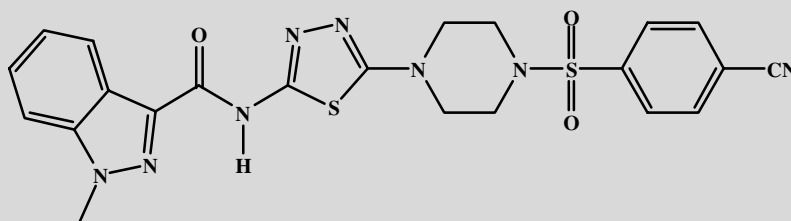
0.47

TD 25



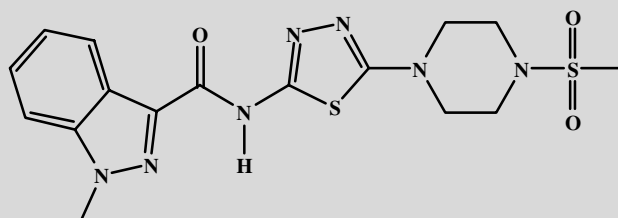
0.81

TD 26



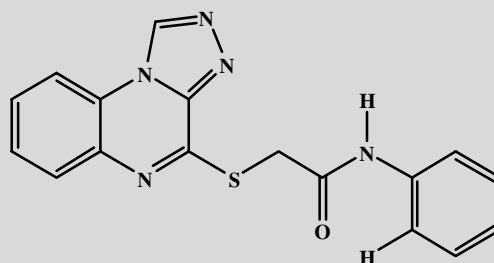
0.74

TD 27



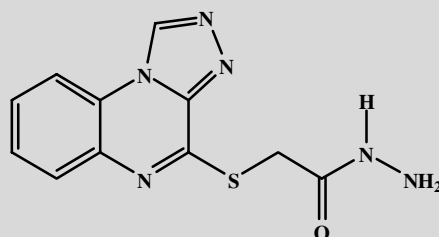
0.91

TD 28



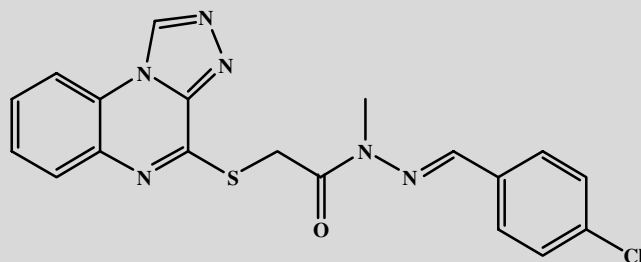
1.60

TD 29



1.90

TD 37



1.90

TABLE-2
VALUES OF TOPOLOGICAL DESCRIPTORS OF THIADIAZOLE AND
QUINOXALINE DERIVATIVES ALONG WITH ANTIPILEPTIC ACTIVITY

Compound	Molar refractivity	Shape index (basic kappa)			Valence connectivity index (standard)			Activity
		Order 1	Order 2	Order 3	Order 0	Order 1	Order 2	
TD 1	134.579	26.601	12.240	6.533	20.114	13.077	10.610	0.810
TD 2	119.525	24.135	10.508	5.742	18.650	11.833	9.957	0.870
TD 3	92.246	18.781	8.131	5.019	14.534	9.839	8.154	0.910
TD 4	117.390	23.168	9.868	5.333	18.988	12.281	11.162	0.300
TD 5	171.721	33.161	13.278	5.781	26.567	18.179	15.967	0.830
TD 6	105.816	22.203	9.647	5.087	16.851	10.775	8.952	0.540
TD 7	121.390	29.970	11.852	7.398	19.918	12.461	10.461	0.240
TD 8	114.484	23.168	10.292	5.689	17.727	11.416	9.533	0.900
TD 9	103.469	21.703	8.789	5.136	16.918	10.595	10.585	0.900
TD 10	115.416	26.074	10.948	6.416	18.361	11.733	9.745	0.400
TD 11	121.851	23.168	10.292	5.689	19.263	12.184	10.419	0.670
TD 12	117.065	23.168	10.292	5.689	18.691	11.898	10.089	0.910
TD 13	122.741	28.994	12.027	6.966	19.548	12.239	10.125	0.320
TD 15	115.416	26.074	10.948	6.416	18.361	11.733	9.742	0.470
TD 16	141.967	31.426	12.545	6.745	22.125	13.790	11.524	0.330
TD 17	140.616	32.395	12.416	7.131	22.495	14.012	11.860	0.250
TD 18	194.884	36.950	15.264	7.275	29.067	19.385	16.499	0.810
TD 19	136.616	25.641	10.401	5.218	21.565	13.832	12.561	0.320
TD 20	141.076	25.641	10.776	5.496	21.840	13.736	11.818	0.800
TD 21	136.291	25.641	10.776	5.496	21.269	13.450	11.488	0.790
TD 22	133.709	25.641	10.776	5.496	20.305	12.968	10.931	0.840
TD 24	134.642	28.526	11.472	6.189	20.939	13.285	11.140	0.470
TD 25	134.642	28.526	11.472	6.189	20.939	13.285	11.144	0.810
TD 26	134.406	26.601	11.396	5.723	20.252	12.941	10.754	0.740
TD 27	108.891	21.240	8.626	4.694	16.995	11.259	9.421	0.910
TD 28	94.726	17.416	8.131	4.066	13.402	8.359	6.097	1.600
TD 29	74.536	13.959	6.185	2.880	10.593	6.487	4.750	1.900
TD 30	91.476	17.416	7.319	3.486	13.525	8.230	6.294	1.600
TD 31	107.504	21.240	10.347	5.587	16.037	10.257	7.665	1.500
TD 32	98.511	18.781	9.087	4.803	14.448	8.621	6.124	1.500
TD 33	112.055	21.240	10.347	5.587	16.127	9.721	7.085	1.500
TD 34	82.918	16.844	7.713	4.110	12.424	7.402	5.412	1.500
TD 35	104.664	19.322	9.467	4.899	14.427	8.879	6.387	1.600
TD 36	106.358	20.280	9.667	5.136	14.797	9.013	6.571	1.600

regression coefficient becomes unity. QSAR model has no predictive power if either the value of cross-validation coefficient (rCV^2) is less than 0.2 or the value regression coefficient (r^2) is less than 0.5. Predicted antiepileptic activities PB1-PB8 of the compounds have been obtained by substituting the values of descriptors in the MLR equations and are given in Table-3.

Out of 90 QSAR models developed with the help of topological descriptors, the good QSAR models are 80. Five good QSAR models in decreasing order of predicted epileptic activity are listed in Table-4 along with the descriptors used. These good QSAR models are PB1, PB2, PB3, PB4 and PB5 in the decreasing order of their predictive power.

Description of first five good QSAR models

Best QSAR model: The best QSAR model is PB1 in which the descriptors are molar refractivity, shape index (basic kappa, order 1), shape index (basic kappa, order 3) and valence connectivity index (order 0, standard). Multi linear regression (MLR) equation is given below:

$$PB1 = 0.0585933 * \text{Molar refractivity} - 0.0187282 * \text{Shape index (basic kappa, order 1)} - 0.111044 * \text{Shape index (basic kappa, order 3)} - 0.392556 * \text{Valence connectivity index (order 0, standard)} + 2.18438$$

$$rCV^2 = 0.832189$$

$$r^2 = 0.872435$$

TABLE-3
VALUES OF THE PREDICTED ANTIEPILEPTIC ACTIVITIES FROM PB1-PB8

Compound	PB1	PB2	PB3	PB4	PB5	PB6	PB7	PB8
TD 1	0.950	0.938	0.940	0.929	0.931	0.740	0.787	0.561
TD 2	0.777	0.767	0.765	0.765	0.765	0.907	0.870	0.836
TD 3	0.975	0.929	0.980	0.955	0.957	1.271	1.099	1.087
TD 4	0.583	0.568	0.566	0.562	0.563	0.973	0.717	0.978
TD 5	0.554	0.615	0.595	0.578	0.579	0.294	0.106	0.822
TD 6	0.789	0.824	0.798	0.796	0.795	1.038	0.998	1.063
TD 7	0.095	0.108	0.112	0.114	0.113	0.511	0.806	0.260
TD 8	0.868	0.857	0.861	0.854	0.855	0.973	0.924	0.854
TD 9	0.629	0.611	0.620	0.620	0.623	1.072	0.790	1.046
TD 10	0.538	0.548	0.549	0.544	0.544	0.776	0.897	0.602
TD 11	0.697	0.650	0.656	0.659	0.659	0.973	0.811	0.854
TD 12	0.641	0.618	0.613	0.613	0.613	0.973	0.853	0.854
TD 13	0.386	0.425	0.405	0.407	0.407	0.577	0.849	0.410
TD 15	0.538	0.548	0.549	0.544	0.544	0.776	0.897	0.602
TD 16	0.480	0.520	0.500	0.512	0.511	0.412	0.671	0.487
TD 17	0.194	0.215	0.214	0.226	0.224	0.346	0.628	0.353
TD 18	0.693	0.681	0.699	0.691	0.692	0.037	0.038	0.303
TD 19	0.664	0.642	0.646	0.652	0.652	0.805	0.539	1.018
TD 20	0.787	0.737	0.747	0.761	0.759	0.805	0.633	0.921
TD 21	0.730	0.705	0.704	0.714	0.713	0.805	0.675	0.921
TD 22	0.957	0.944	0.952	0.955	0.955	0.805	0.746	0.921
TD 24	0.632	0.644	0.645	0.649	0.649	0.609	0.720	0.680
TD 25	0.632	0.644	0.645	0.649	0.649	0.609	0.719	0.680
TD 26	0.976	0.992	0.982	0.984	0.984	0.740	0.769	0.842
TD 27	0.974	0.952	0.985	0.973	0.974	1.104	0.938	1.200
TD 28	1.696	1.702	1.706	1.704	1.704	1.364	1.361	1.418
TD 29	1.812	1.853	1.846	1.846	1.846	1.599	1.532	1.830
TD 30	1.522	1.552	1.543	1.551	1.550	1.364	1.336	1.619
TD 31	1.170	1.170	1.160	1.152	1.152	1.104	1.162	0.889
TD 32	1.400	1.399	1.382	1.392	1.390	1.271	1.358	1.162
TD 33	1.401	1.378	1.374	1.382	1.381	1.104	1.235	0.889
TD 34	1.394	1.420	1.402	1.408	1.407	1.403	1.448	1.403
TD 35	1.748	1.738	1.744	1.743	1.744	1.234	1.324	1.128
TD 36	1.657	1.646	1.655	1.656	1.657	1.169	1.301	1.046

TABLE-4
GOOD QSAR MODELS IN THE DECREASING ORDER OF PREDICTIVE
EPILEPTIC ACTIVITIES ALONG WITH THE DESCRIPTORS USED

Predicted activity	Descriptors used in the predicted activity	Cross-validation coefficient (rCV ²)	Regression coefficient (r ²)
PB1	Molar refractivity, shape index (basic kappa, order 1), shape index (basic kappa, order 3), valence connectivity index (order 0, standard)	0.832189	0.872435
PB2	Molar refractivity, shape index (basic kappa, order 2), shape index (basic kappa, order 3), valence connectivity index (order 0, standard)	0.787784	0.871703
PB3	Molar refractivity, shape index (basic kappa, order 3), valence connectivity index (order 0, standard), valence connectivity index (order 1, standard)	0.813375	0.871128
PB4	Molar refractivity, shape index (basic kappa, order 3), valence connectivity index (order 0, standard), valence connectivity index (order 2, standard)	0.800679	0.870877
PB5	Molar refractivity, shape index (basic kappa, order 3), valence connectivity index (order 0, standard)	0.829812	0.870871

The value of regression coefficient is 0.872435 and the value of cross-validation coefficient is 0.872435. These values of regression and cross-validation coefficients indicate that the QSAR model possesses very good predictive power and can be used to predict the antiepileptic activity of any compound of this series. Graph between observed and predicted antiepileptic activities is shown in Fig. 1. The difference between observed antiepileptic activity and predicted antiepileptic activity PB1 is shown in Fig. 2.

Second best QSAR model: The second best QSAR model is PB2 whose MLR equation is given by:

$$\text{PB2} = 0.0532403 * \text{Molar refractivity} + 0.060905 * \text{Shape index (basic kappa, order 2)} - 0.208831 * \text{Shape index (basic kappa, order 3)} - 0.390519 * \text{Valence connectivity index (order 0, standard)} + 2.24621$$

$$rCV^2 = 0.787784$$

$$r^2 = 0.871703$$

These values of regression and cross-validation coefficients indicate that this QSAR model possesses very good predictive power and can be used to predict the antiepileptic activity of any compound of this series. Graph between observed and predicted antiepileptic activities is shown in Fig. 3. The

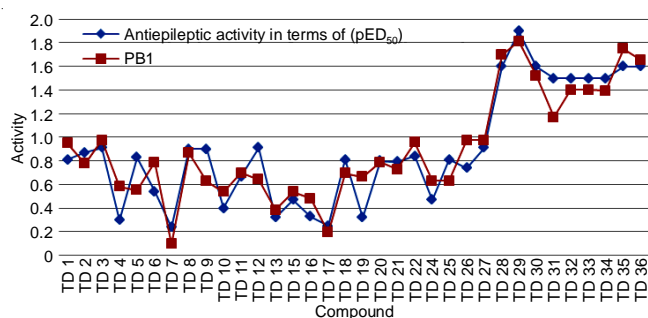


Fig. 1. Graph between observed activity and predicted activity PB1

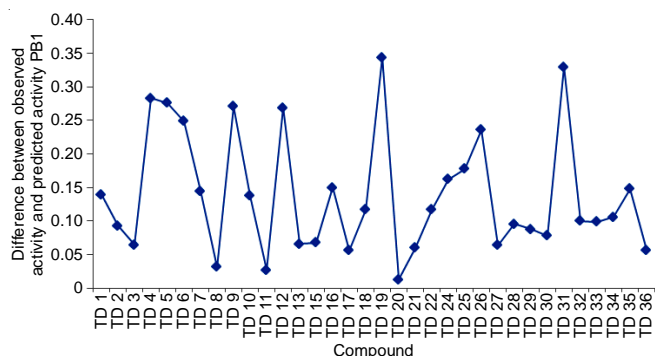


Fig. 2. Graph showing the difference between observed activity and predicted activity PB1

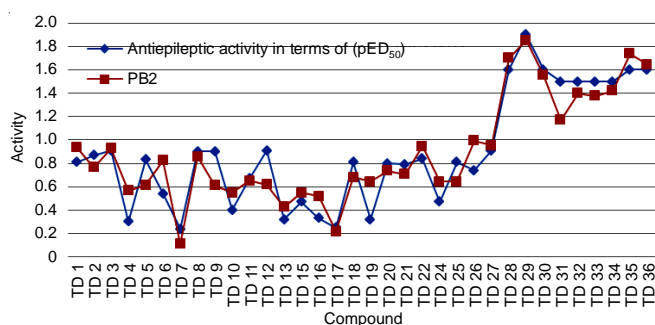


Fig. 3. Graph between observed activity and predicted activity PB2

difference between observed antiepileptic activity and predicted antiepileptic activity PB2 is shown in Fig. 4.

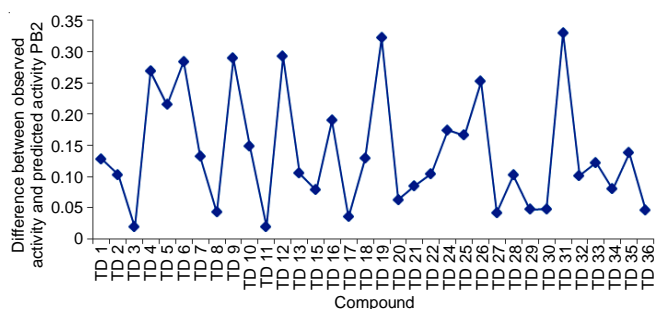


Fig. 4. Graph showing the difference between observed activity and predicted activity PB2

Third best QSAR model: The third best QSAR model is PB3 whose MLR equation is given by:

$$\text{PB3} = 0.0585114 * \text{Molar refractivity} - 0.142787 * \text{Shape index (basic kappa, order 3)} - 0.42761 * \text{Valence Connectivity index (order 0, standard)} + 0.0262424 * \text{Valence connectivity index (order 1, standard)} + 2.25573$$

$$rCV^2 = 0.813375$$

$$r^2 = 0.871128$$

These values of regression and cross-validation coefficients indicate that this QSAR model possesses very good predictive power and can be used to predict the antiepileptic activity of any compound of this series. Graph between observed and predicted antiepileptic activities is shown in Fig. 5. The difference between observed antiepileptic activity and predicted antiepileptic activity PB3 is shown in Fig. 6.

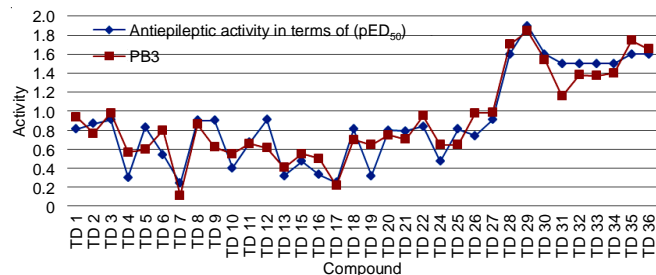


Fig. 5. Graph between observed activity and predicted activity PB3

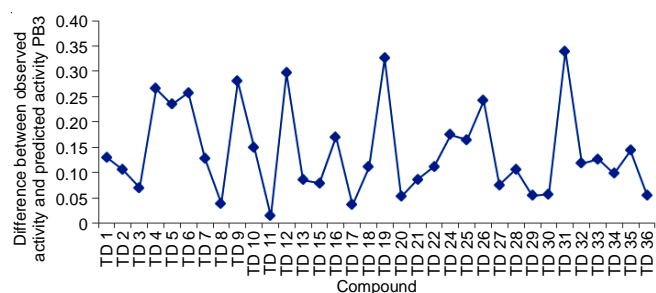


Fig. 6. Graph showing the difference between observed activity and predicted activity PB3

Fourth best QSAR model: The fourth best QSAR model is PB4 whose MLR equation is given by:

$$\text{PB4} = 0.0581155 * \text{Molar refractivity} - 0.14874 * \text{Shape index (basic kappa, order 3)} - 0.403869 * \text{Valence connectivity index (order 0, standard)} - 0.00291618 * \text{Valence connectivity index (order 2, standard)} + 2.2343$$

$$rCV^2 = 0.800679$$

$$r^2 = 0.870877$$

These values of regression and cross-validation coefficients indicate that this QSAR model possesses very good predictive power and can be used to predict the antiepileptic activity of any compound of this series. Graph between observed and predicted antiepileptic activities is shown Fig. 7. The difference between observed antiepileptic activity and predicted antiepileptic activity PB4 is shown in Fig. 8.

Fifth best QSAR model: The Fifth best QSAR model is PB5 whose MLR equation is given by:

$$\text{PB5} = 0.0583898 * \text{Molar refractivity} - 0.147308 * \text{Shape index (basic kappa, order 3)} - 0.407782 * \text{Valence connectivity index (order 0, standard)} + 2.2373$$

$$rCV^2 = 0.829812$$

$$r^2 = 0.870871$$

These values of regression and cross-validation coefficients indicate that this QSAR model possesses very good

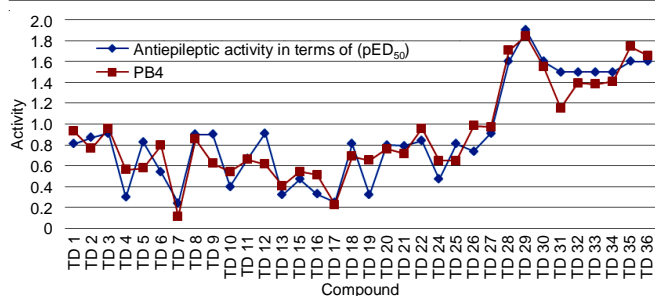


Fig. 7. Graph between observed activity and predicted activity PB4

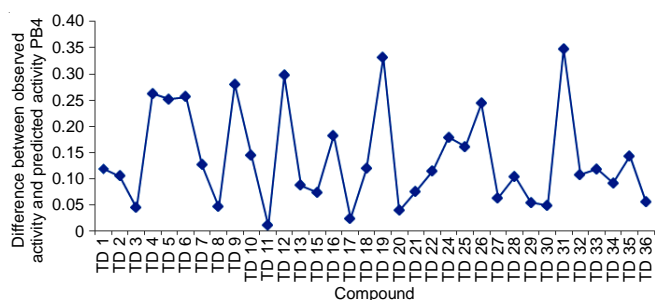


Fig. 8. Graph showing the difference between observed activity and predicted activity PB4

predictive power and can be used to predict the antiepileptic activity of any compound of this series.

Good QSAR model using single descriptors:

Descriptors shape index (basic kappa, order 1), valence connectivity index (order 2, standard) and shape index (basic kappa, order 3) are individually capable to produce good QSAR models. These QSAR models are discussed below:

QSAR model using single descriptor shape index (basic kappa, order 1): The predicted activity PB6 of the QSAR model developed using the descriptor Shape Index (basic kappa, order 1) is as follows-

$$\begin{aligned} \text{PB6} &= -0.0679319 * \text{Shape Index (basic kappa, order 1)} + 2.54677 \\ r\text{CV}^2 &= 0.515348 \\ r^2 &= 0.536487 \end{aligned}$$

The values of regression and cross-validation coefficients suggest that the QSAR model possesses good predictive power.

QSAR model using single descriptor valence connectivity index (order 2, standard): The predicted activity PB7 of the QSAR model developed using the descriptor Valence Connectivity Index (order 2, standard) is as follows-

$$\begin{aligned} \text{PB7} &= -0.127179 * \text{Valence connectivity index (order 2, standard)} + 2.13646 \\ r\text{CV}^2 &= 0.476899 \\ r^2 &= 0.509596 \end{aligned}$$

The values of regression and cross-validation coefficients suggest that the QSAR model possesses good predictive power.

QSAR model using single descriptor shape index (basic kappa, order 2): The predicted activity PB8 of the QSAR model developed using the descriptor shape index (basic kappa, order 3) is as follows:

$$\begin{aligned} \text{PB8} &= -0.347358 * \text{Shape index (basic kappa, order 3)} + 2.83016 \\ r\text{CV}^2 &= 0.522455 \\ r^2 &= 0.549397 \end{aligned}$$

The values of regression and cross-validation coefficients suggest that the QSAR model possesses good predictive power.

Conclusion

Best QSAR model is PB1 in which the descriptors are molar refractivity, shape index (basic kappa, order 1), shape index (basic kappa, order 3) and valence connectivity index (order 0, standard). In this QSAR model, the regression coefficient is 0.872435 and cross-validation coefficient is 0.832189. These values of regression and cross-validation coefficients indicate that the predictive power of the QSAR model PB1 is excellent. Shape index (basic kappa, order 1) alone produces QSAR model having good predictive power in which regression and cross-validation coefficients are 0.515348 and 0.536487 respectively. The single descriptor shape index (basic kappa, order 3) and the single descriptor valence connectivity index (order 2, standard) also produce the QSAR models having good predictive power.

REFERENCES

- S. Kwon, H. Bae, J. Jo and S. Yoon, Comprehensive Ensemble in QSAR Prediction for Drug Discovery, *BMC Bioinformatics*, **20**, 521 (2019); <https://doi.org/10.1186/s12859-019-3135-4>
- P.P. Singh, F.A. Pasha and H.K. Srivastava, DFT Based Atomic Softness and Its Application in Site Selectivity, *QSAR Comb. Sci.*, **22**, 843 (2003); <https://doi.org/10.1002/qsar.200330828>
- F.A. Pasha, H.K. Srivastava and P.P. Singh, Semiempirical QSAR study and Ligand Receptor Interaction of Estrogens, *J. Mol. Div.*, **9**, 215 (2005); <https://doi.org/10.1007/s11030-005-2711-x>
- P.P. Singh, F.A. Pasha and H.K. Srivastava, QSAR Study of Estrogens with the Help of PM3-based Descriptors, *Int. J. Quan. Chem.*, **104**, 87 (2005); <https://doi.org/10.1002/qua.20569>
- P.P. Singh, F.A. Pasha and H.K. Srivastava, Novel Application of Softness Parameter for Regioselectivity and Reaction Mechanism, *Indian J. Chem.*, **43B**, 983 (2004).
- P.P. Singh, H.K. Srivastava and F.A. Pasha, DFT-based QSAR study of Testosterone and its Derivatives, *Bioorg. Med. Chem.*, **12**, 171 (2004); <https://doi.org/10.1016/j.bmc.2003.11.002>
- B.R. Allen and S.Y. Stanley, An Introduction to QSAR Methodology, C.S.J. Walpole, R. Wrigglesworth, S. Bevan, E.A. Campbell, A. Dray, I.F. James, K.J. Masdin, M.N. Perkins and J. Winter, Analogs of Capsaicin with Agonist Activity as Novel Analgesic Agents; Structure-Activity Studies. 3. The Hydrophobic Side-Chain "C-region", *J. Med. Chem.*, **36**, 2381 (1993); <https://doi.org/10.1021/jm00068a016>
- J.G. Topliss, Utilization of Operational Schemes for Analog Synthesis in Drug Design, *J. Med. Chem.*, **15**, 1006 (1972); <https://doi.org/10.1021/jm00280a002>
- Y.C. Martin, A Practitioner's Perspective of the Role of Quantitative Structure-Activity Analysis in Medicinal Chemistry, *J. Med. Chem.*, **24**, 229 (1981); <https://doi.org/10.1021/jm00135a001>
- G.T. John, Quantitative Structure-Activity Relationships of Drugs, Academic Press: New York (1983).
- R. Franke, Theoretical Drug Design Methods, Elsevier: Amsterdam, (1984).
- H.-H. Hsu, C.-H. Huang and S.-T. Lin, New Data Structure for Computational Molecular Design with Atomic or Fragment Resolution, *J. Chem. Inf. Model.*, **59**, 3703 (2019); <https://doi.org/10.1021/acs.jcim.9b00478>
- H.C. Neu, Quinolones Revisited: Where are We? *Antimicrob. Newslett.*, **4**, 9 (1987); [https://doi.org/10.1016/0738-1751\(87\)90008-6](https://doi.org/10.1016/0738-1751(87)90008-6)
- P.B. Fernandes, Mode of Action, and *in vitro* and *in vivo* Activities of the Fluoroquinolones, *J. Clin. Pharmacol.*, **28**, 156 (1987); <https://doi.org/10.1002/j.1552-4604.1988.tb05967.x>

16. P.G. Drake and B.I. Posner, Insulin Receptor-Associated Protein Tyrosine Phosphatase(s): Role in Insulin Action, *Mol. Cell. Biochem.*, **182**, 79 (1998);
<https://doi.org/10.1023/A:1006808100755>
17. M.F. White and C.R. Kahn, The Insulin Signaling System, *J. Biol. Chem.*, **269**, 1 (1994);
[https://doi.org/10.1016/S0021-9258\(17\)42297-6](https://doi.org/10.1016/S0021-9258(17)42297-6)
18. H. Byon, A.B. Kusari and J. Kusari, Protein-Tyrosine Phosphatase-1B Acts as a Negative Regulator of Insulin Signal Transduction, *Mol. Cell. Biochem.*, **182**, 101 (1998);
<https://doi.org/10.1023/A:1006868409841>
19. F. Ahmad, P.-M. Li, J. Meyerovitch and B.J. Goldstein, Smotic Loading of Neutralizing Antibodies Demonstrates a Role for Protein-tyrosine Phosphatase 1B in Negative Regulation of the Insulin Action Pathway, *J. Biol. Chem.*, **270**, 20503 (1995);
<https://doi.org/10.1074/jbc.270.35.20503>
20. D. Bandyopadhyay, A. Kusari, K.A. Kenner, F. Liu, J. Chernoff, T.A. Gustafson and J. Kusari, Protein-Tyrosine Phosphatase 1B Complexes with the Insulin Receptor *in vivo* and Is Tyrosine-phosphorylated in the Presence of Insulin, *J. Biol. Chem.*, **272**, 1639 (1997);
<https://doi.org/10.1074/jbc.272.3.1639>
21. J. Kusari, K.A. Kenner, K.I. Suh, D.E. Hill and R.R. Henry, Skeletal Muscle Protein Tyrosine Phosphatase Activity and Tyrosine Phosphatase 1B Protein Content are Associated with Insulin Action and Resistance, *J. Clin. Invest.*, **93**, 1156 (1994);
<https://doi.org/10.1172/JCI117068>
22. J.B. Stanbury, J.B. Wyngaarden and D.S. Fredrickson, The Metabolic Basis of Inherited Disease, McGraw-Hill: New York, p. 182 (1978).
23. R.G. Parr, R.A. Donnelly, M. Levy and W.E. Palke, Electronegativity: The Density Functional Viewpoint, *J. Chem. Phys.*, **68**, 3801 (1978);
<https://doi.org/10.1063/1.436185>
24. M.C. Flanigan, A. Komornicki and J.W. McIver, Modern Theoretical Chemistry, Plenum Press: New York, vol. 8 (1977).
25. M.J.S. Dewar and H.S. Rzepa, Ground States of Molecules. 45. MNDO Results for Molecules Containing Beryllium, *J. Am. Chem. Soc.*, **100**, 777 (1978);
<https://doi.org/10.1021/ja00471a020>
26. B. Lee and E.M. Richards, The Interpretation of Protein Structures: Estimation of Static Accessibility, *J. Mol. Biol.*, **55**, 379 (1971);
[https://doi.org/10.1016/0022-2836\(71\)90324-X](https://doi.org/10.1016/0022-2836(71)90324-X)
27. L.B. Kier, Distinguishing Atom Differences in a Molecular Graph Shape Index, *Quant. Struct.-Act. Relat.*, **5**, 7 (1986);
<https://doi.org/10.1002/qsar.19860050103>
28. L.B. Kier, Indexes of Molecular Shape from Chemical Graphs, *Med. Res. Rev.*, **7**, 417 (1987);
<https://doi.org/10.1002/med.2610070404>
29. R.G. Parr and W. Yang, Density Functional Theory of Atoms and Molecules, Oxford University Press: New York (1989).
30. J.J.P. Stewart, Optimization of Parameters for Semiempirical Methods I. Method, *J. Comput. Chem.*, **10**, 209 (1989);
<https://doi.org/10.1002/jcc.540100208>
31. Z. Mihalic, D. Veljan, D. Amic, S. Nikolic, D. Plavsic and N. Trinajstic, The Distance Matrix in Chemistry, *J. Math. Chem.*, **11**, 223 (1992);
<https://doi.org/10.1007/BF01164206>
32. H. Haruo, Topological Index. A Newly Proposed Quantity Characterizing the Topological Nature of Structural Isomers of Saturated Hydrocarbons, *Bull. Chem. Soc. Jpn.*, **44**, 2332 (1971);
<https://doi.org/10.1246/bcsj.44.2332>
33. M. Barysz, G. Jashari, R.S. Lall, V. Srivastava and N.K. Trinajstic, Eds.: R.B. King, On the Distance Matrix of Molecules Containing Heteroatoms; In: Chemical Applications of Topology and Graph Theory, Elsevier: Amsterdam, pp. 222-230 (1983).
34. M. Randic, Characterization of Molecular Branching, *J. Am. Chem. Soc.*, **97**, 6609 (1975);
<https://doi.org/10.1021/ja00856a001>
35. L.B. Kier, L.H. Hall, W.J. Murray and M. Randic, Molecular Connectivity V: Connectivity Series Concept Applied to Density, *J. Pharm. Sci.*, **65**, 1226 (1976);
<https://doi.org/10.1002/jps.2600650824>